Investigating Quantum Reservoir Computing for Time Series Forecasting

Md Shadnan Azwad Khan, Merve Rumelli, Natalia Capra Ferrazzo
Faculty of Science and Engineering, Sorbonne Université, Paris, France
Email: {md_shadnan_azwad.khan, merve.rumelli, natalia.capra_ferrazzo}@etu.sorbonne-universite.fr

SCIENCES SORBONNE UNIVERSITÉ

Abstract

We investigate Quantum Reservoir Computing (QRC), a quantum adaptation of classical reservoir computing that leverages quantum dynamics for complex temporal learning. Unlike traditional methods that rely on extensive training, QRC uses quantum systems as computational black boxes where only readout layers are trained, simplifying the process significantly. Well suited to the noisy, intermediate-scale quantum (NISQ) era, QRC tolerates the challenges of decoherence while offering promising computational advantages. However, substantial hurdles in design, implementation, and theoretical understanding persist. Our work highlights the mathematical constructs that facilitate QRC's capabilities, focusing on the potential in time-series forecasting.

Introduction

Among the emerging quantum machine learning paradigms, Quantum Reservoir Computing (QRC) stands out by merging the principles of classical reservoir computing (RC) with quantum dynamics. Classical RC, exemplified by models like Echo State Networks (ESNs), efficiently handles temporal data by projecting inputs into a high-dimensional space, requiring minimal training focused solely on output weights [1]. This simplicity offers a stark contrast to the extensive training demands of deep neural networks (DNNs). QRC harnesses the natural evolution of quantum states to process information dynamically [2]. This method reduces the need for extensive computational resources by exploiting quantum mechanical interactions as computational assets. QRC offers a potent alternative for applications requiring time series prediction, such as financial forecasting and weather prediction.

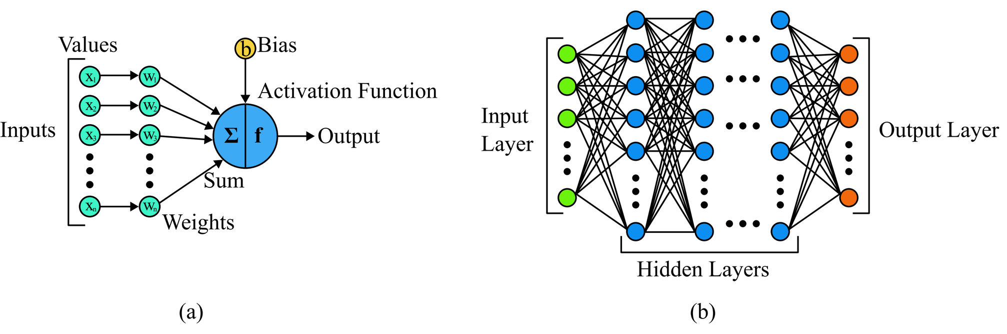

Figure 1: DNN Explained: (a) Diagram of an artificial neuron. (b) Architecture of a typical DNN with multiple interconnected layers

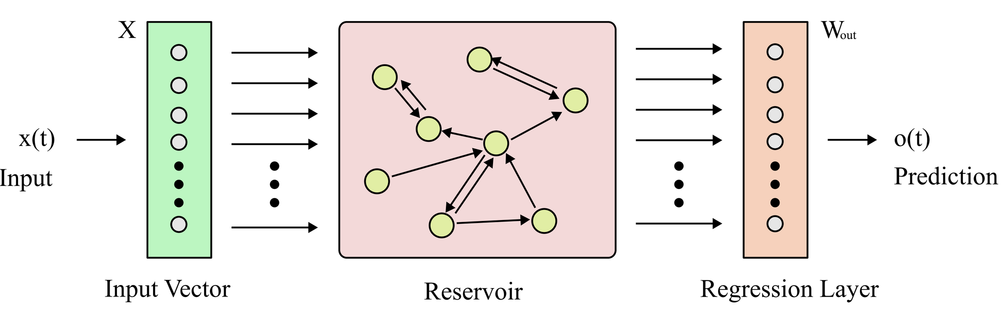

Figure 2: Overview of a Typical ESN: Illustrates how a time series input flows through a fixed, random reservoir and is then processed by a trainable readout layer to generate the output.

Methods

Encoding Classical Data into Quantum States

Classical data vector $\mathbf{x}$ of length $N = 2^n$ (where n is the number of qubits) is encoded into the amplitudes of a quantum state using the relation [3]:

$$|\psi\rangle = \sum_{i=0}^{N-1} x_i |i\rangle, \quad \rho = \sum_k p_k |\psi_k\rangle\langle\psi_k|$$

Here, $|i\rangle$ denotes the computational basis states, and the vector $\mathbf{x}$ is normalized such that $\sum |x_i|^2 = 1$. To account for noise or partial coherence, the state can be represented using a density matrix ρ, where p_k is the probability of the system being in the state $|\psi_k\rangle$.

Quantum Reservoir

The foundational element of QRC is its ability to simulate complex dynamics within a Hilbert space $\mathcal{H}$, governed by unitary transformations $U(t) = e^{-iHt/\hbar}$ that evolve the state $|\psi(t)\rangle$. This allows for the exploration and manipulation of the quantum state across an N-dimensional space using randomly sampled unitary operators from the unitary group $U(N)$, ensuring optimal state adaptability.

Additionally, QRC models include real-world phenomena like noise and decoherence through the Lindblad master equation [4]:

$$\frac{d\rho}{dt} = -\frac{i}{\hbar}[H, \rho] + \sum_k \gamma_k \left(L_k \rho L_k^\dagger - \frac{1}{2}\{L_k^\dagger L_k, \rho\} \right)$$

This equation captures both unitary and non-unitary dynamics, crucial for accurately describing environmental effects on quantum systems. Lindblad operators (L_k) introduce stochastic behaviors and nonlinearities, essential for the reservoir's capability to process complex information and make decisions.

QRC's reliance on the exponential growth of computational states with the increase in qubits, represented as

$$|\psi\rangle = \sum_{q_1,\ldots,q_n=0}^{1} c_{q_1\ldots q_n} |q_1 \ldots q_n\rangle$$

highlights its potential to process information far more efficiently and complexly than classical systems.

Quantum Measurement

The process of decoding and measuring the reservoir outputs involves projecting the quantum state $|\psi\rangle$ onto a predefined set of observable eigenstates $\{|j\rangle\}$, with the output vector $\mathbf{y}(t)$ calculated as:

$$y_j(t) = |\langle j|\psi(t)\rangle|^2, \quad |\psi'\rangle = \frac{P_k|\psi\rangle}{\sqrt{\langle\psi|P_k|\psi\rangle}}$$

The quantum measurement employs orthogonal projection operators $\{P_k\} = |k\rangle\langle k|$, with each measurement collapsing the state and potentially altering its evolution path post measurement.

In the other case, Positive Operator-Valued Measures (POVMs), represented by semi-definite operators $\{E_m\}$, enhances the flexibility of measurement outcomes. The updated state and probabilities under POVM are given by:

$$\rho' = \sum_m M_m \rho M_m^\dagger, \quad p(m) = \mathrm{Tr}(M_m \rho M_m^\dagger)$$

Training and Predictions

Quantum measurements decode the system states into classical outputs $\mathbf{y}(t)$. These outputs are then processed through a linear readout layer. The readout formula is:

$$\mathbf{o}(t) = \mathbf{W}_{out}\mathbf{y}(t) + \mathbf{b}$$

Here, $\mathbf{W}_{out}$ denotes a weight matrix, and $\mathbf{b}$ a bias vector. Training focuses on minimizing the mean squared error $\mathcal{L}$ between the predicted outputs $\mathbf{o}(t)$ and the actual targets $\mathbf{o}_{\text{true}}(t)$:

$$\mathcal{L} = \frac{1}{N}\sum_{t=1}^{N} \|\mathbf{o}(t) - \mathbf{o}_{\text{true}}(t)\|^2$$

Weights are updated via gradient descent:

$$\mathbf{W}_{out}^{(new)} = \mathbf{W}_{out}^{(old)} - \eta \nabla_{\mathbf{W}_{out}} \mathcal{L}, \quad \hat{o}(t) = \mathbf{W}_{out}\mathbf{y}(t)$$

where η is the learning rate. This iterative refinement enhances the model's accuracy and reliability. Once trained, the readout layer predicts future states or outcomes. This final output $\hat{o}(t)$ encapsulates the quantum system's predictions, applicable in time-series forecasting.

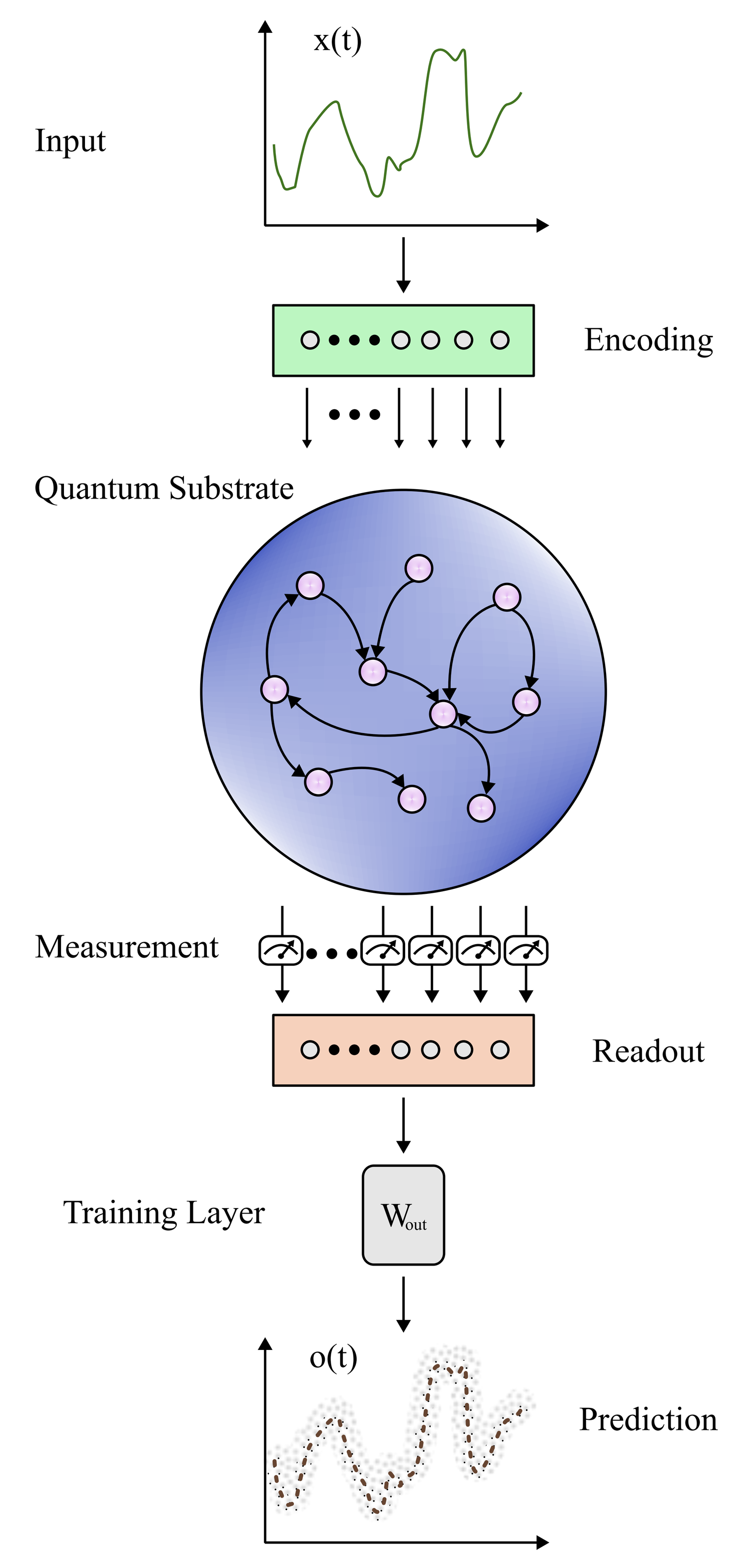

Figure 3: Illustration of the Quantum Reservoir Computing Process.

Implementations

QRC leverages diverse quantum systems to harness unique computational advantages [5]. Nuclear Magnetic Resonance (NMR) in molecules, suited for small-scale prototypes, offers long coherence and precise control [6]. Trapped ions provide scalability and high-fidelity operations, suitable for intricate QRC applications [7]. Fermion and Boson lattices allow flexible manipulation of quantum statistical models [8], while superconducting qubits integrate seamlessly with electronic circuits, facilitating rapid processing [9]. Quantum circuits, designed with various gates, customize reservoir computing dynamics [10]. Photonics leverages light's quantum states for high-speed, energy-efficient computing, ideal for scalable optical systems [11]. Simulation platforms such as Qiskit [12] are essential for designing, simulating, and refining QRC models, enhancing their applicability across various scientific and technological domains.

Benchmarking

NARMA Series Prediction

The NARMA task tests the system's capability to predict highly nonlinear behaviors:

$$y(t+1) = ay(t) + by(t)\sum_{i=0}^{n-1} y(t-i) + cu(t-n+1)u(t) + d$$

where $u(t)$ is the input and $y(t)$ the output.

Mackey-Glass Time Series Prediction

This benchmark assesses QRC's performance in chaotic time series prediction using the differential equation:

$$\frac{dx(t)}{dt} = \beta \frac{x(t-\tau)}{1 + x(t-\tau)^n} - \gamma x(t)$$

It requires QRC to predict future values $x(t)$.

Lorenz Time Series Prediction

The Lorenz system, a set of three chaotic differential equations, examines QRC's dynamical modeling capabilities:

$$\left(\frac{dx}{dt}, \frac{dy}{dt}, \frac{dz}{dt}\right) = (\sigma(y - x), x(\rho - z) - y, xy - \beta z)$$

Performance Metrics

Performance can be quantified using:

Mean Squared Error (MSE):

$$\mathrm{MSE} = \frac{1}{N}\sum_{t=1}^{N}(y(t) - \hat{y}(t))^2$$

Normalized MSE (NMSE):

$$\mathrm{NMSE} = \frac{\mathrm{MSE}}{\mathrm{Var}(y)}$$

Normalized Root MSE (NRMSE):

$$\mathrm{NRMSE} = \sqrt{\frac{\mathrm{MSE}}{\mathrm{Var}(y)}}$$

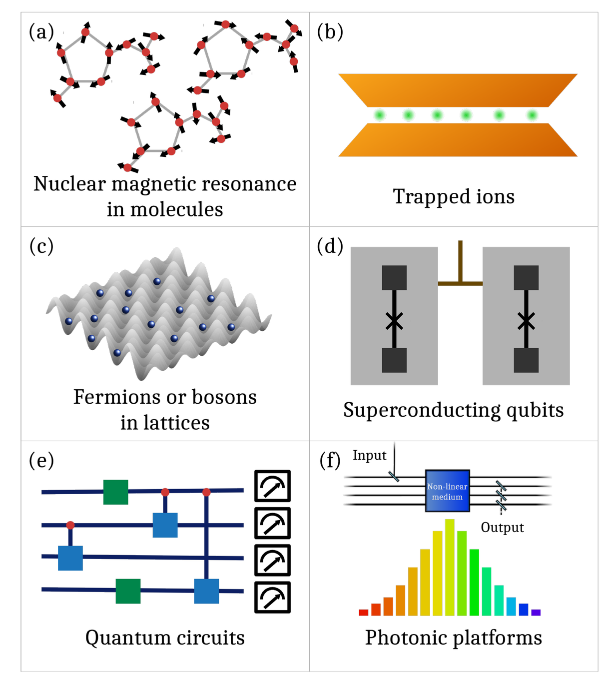

Figure 4: Various viable QRC Substrate types (a)-(f) [5].

Conclusion

Our discussions have addressed both theoretical aspects and potential practical applications of QRC, underscoring its prospective advantages over traditional computational models through theoretical analyses and preliminary benchmarks, such as tasks involving NARMA processing and Mackey-Glass series predictions. Despite these promising discussions, empirical validation through rigorous simulations and benchmarking remains pending. Future work could further illuminate QRC's capacity for complex pattern recognition and dynamic system modeling.

References

[1] Mantas Lukoševičius. A practical guide to applying echo state networks. In *Neural Networks: Tricks of the Trade: Second Edition*, pages 659–686. Springer, 2012.

[2] Keisuke Fujii and Kohei Nakajima. Harnessing disordered-ensemble quantum dynamics for machine learning. *Physical Review Applied*, 8(2): 024030, 2017.

[3] Manuela Weigold, Johanna Barzen, Frank Leymann, and Marie Salm. Data encoding patterns for quantum computing. In *Proceedings of the 27th Conference on Pattern Languages of Programs*, pages 1–11, 2020.

[4] DN Bernal-Garcia, L Huang, AE Miroshnichenko, and MJ Wooley. Generalized lindblad master equations in quantum reservoir engineering. *arXiv preprint arXiv:2111.04041*, 2022.

[5] Pere Mujal, Rodrigo Martínez-Peña, Johannes Nokkala, Jorge García-Beni, Gian Luca Giorgi, Miguel C Soriano, and Roberta Zambrini. Opportunities in quantum reservoir computing and extreme learning machines. *Advanced Quantum Technologies*, 4(8):2100027, 2021.

[6] Makoto Negoro, Kosuke Mitarai, Keisuke Fujii, Kohei Nakajima, and Masahiro Kitagawa. Machine learning with controllable quantum dynamics of a nuclear spin ensemble in a solid. *arXiv preprint arXiv:1806.10910*, 2018.

[7] Juan M Pino, Jennifer M Dreiling, Caroline Figgatt, John P Gaebler, Steven A Moses, MS Allman, CH Baldwin, Michael Foss-Feig, D Hayes, K Mayer, et al. Demonstration of the trapped-ion quantum ccd computer architecture. *Nature*, 592(7853):209–213, 2021.

[8] Sanjib Ghosh, Andrzej Opala, Michał Matuszewski, Tomasz Paterek, and Timothy CH Liew. Quantum reservoir processing. *npj Quantum Information*, 5(1):35, 2019.

[9] Philip Krantz, Morten Kjaergaard, Fei Yan, Terry P Orlando, Simon Gustavsson, and William D Oliver. A quantum engineer's guide to superconducting qubits. *Applied physics reviews*, 6(2), 2019.

[10] Sanjib Ghosh, Tanjung Krisnanda, Tomasz Paterek, and Timothy CH Liew. Realising and compressing quantum circuits with quantum reservoir computing. *Communications Physics*, 4(1):105, 2021.

[11] Rohit K Ramakrishnan, Aravinth Balaji Ravichandran, Arpita Mishra, Archana Kaushalram, Gopalkrishna Hegde, Srinivas Talabattula, and Peter P Rohde. Integrated photonic platforms for quantum technology: a review. *ISSS Journal of Micro and Smart Systems*, 12(2):83–104, 2023.

[12] Qiskit contributors. Qiskit: An open-source framework for quantum computing, 2023.